arXiv:0811.3001v2 [hep-ph] 4 Dec 2008

The AdS/QCD Correspondence: Still Undelivered

Csaba Csáki[a], **Matthew Reece**[b], and **John Terning**[c]

[a] *Institute for High Energy Phenomenology*
Newman Laboratory of Elementary Particle Physics
Cornell University, Ithaca, NY 14853, USA

[b] *Princeton Center for Theoretical Science*
Princeton University, Princeton, NJ 08544, USA

[c] *Department of Physics, University of California, Davis, CA 95616.*

csaki@lepp.cornell.edu, mreece@princeton.edu, jterning@gmail.com

Abstract

We consider the particle spectrum and event shapes in large N gauge theories in different regimes of the short-distance 't Hooft coupling, λ. The mesons in the small λ limit should have a Regge spectrum in order to agree with perturbation theory, while generically the large λ theories with gravity duals produce spectra reminiscent of KK modes. We argue that these KK-like states are qualitatively different from QCD modes: they are deeply bound states which are sensitive to short distance interactions rather than the flux tube-like states expected in asymptotically free, confining gauge theories. In addition, we also find that the characteristic event shapes for the large λ theories with gravity duals are close to spherical, very different from QCD-like (small λ, small N) and Nambu-Goto-like (small λ, large N) theories which have jets. This observation is in agreement with the conjecture of Strassler on event shapes in large 't Hooft coupling theories, which was recently proved by Hofman and Maldacena for the conformal case. This conclusion does not change even when considering soft-wall backgrounds for the gravity dual. The picture that emerges is the following: theories with small and large λ are qualitatively different, while theories with small and large N are qualitatively similar. Thus it seems that it is the relative smallness of the 't Hooft coupling in QCD that prevents a reliable AdS/QCD correspondence from emerging, and that reproducing characteristic QCD-like behavior will require genuine stringy dynamics to be incorporated into any putative dual theory.

1 Introduction

Confining gauge theories play a central role in particle physics: they provide the real theory of strong interactions (QCD), and possible models of dynamical electroweak symmetry breaking (EWSB) and dynamical supersymmetry breaking. With the help of the anti-de Sitter/conformal field theory (AdS/CFT) correspondence many of the qualitative features of confining gauge theories can be explained, and warped extra dimensional theories have been used to parametrize strongly coupled, almost conformal, models of dynamical EWSB. The AdS/CFT analogy [1] has been pushed so far as to suggest that most properties of QCD can be understood even quantitatively using a simple Randall-Sundrum (RS)-type extra dimensional model called AdS/QCD: a warped extra dimension with UV and IR cut-off branes, and bulk fields appropriate for the chiral symmetries of QCD [2]. While many results show a surprisingly good agreement ($\mathcal{O}(5-10)\%$) with the QCD data, it always has been a central question whether this agreement is merely the result of properly incorporating chiral symmetries, or if there is some deeper, underlying reason. One recent development that suggests that AdS/QCD is actually not that similar to real QCD is the conjecture of Strassler that event shapes in theories at large 't Hooft coupling are spherical [3]. This possibility was already strongly suggested by the result of Polchinski and Strassler that in hadrons at large 't Hooft coupling, all partons are at small-x ("wee") [4]; thus a parton shower with highly energetic partons is very unlikely. The spherical-event conjecture was proven by Hofman and Maldacena, who in a pioneering work set out to understand the collider physics of conformal theories with a gravity dual [5]. What they found confirmed that these theories behave very differently from QCD: instead of jet-like events one finds energies that are distributed in a spherically symmetric way in the calorimeter. For related work see [6] and also [7]. One aim of this paper is to verify that the results of Hofman and Maldacena persist in the case of a theory with conformal symmetry broken in the IR as in the case of AdS/QCD. Indeed we find that introducing the IR cutoff does not substantially modify the basic results, and generic scattering processes in AdS/QCD-like theories will lead to events with large sphericities (as opposed to jet-like events in QCD). Of course this result is not the first qualitative disagreement between AdS/QCD and real QCD: the resonance spectrum of a simple extra dimensional model is also quite different from QCD, unless a soft-wall metric is assumed for the 5D background. We have checked that the spherical nature of the event shapes persists even when the simple RS background is replaced by the soft-wall background. These results suggest that there is a real disagreement between theories with a gravity dual and QCD, as one would have expected from the beginning since gravity duals are only calculable in theories with large 't Hooft coupling.

In order to better understand what these differences can be let us be more specific and consider QCD as a function of the number of colors N and the 't Hooft coupling $\lambda = g^2 N$. In particular, we are concerned mostly with the value of λ at distances much shorter than the confinement scale, so that by "small λ" we mean asymptotically free or at least asymptotically weak coupling (e.g. a theory with a Banks-Zaks fixed point in the UV). A brief survey of the (N, λ) plane is illustrated in Fig. 1. At large N, and for any λ, we expect a theory with some stringy reorganization in a $1/N$ expansion [8] (but not necessarily a

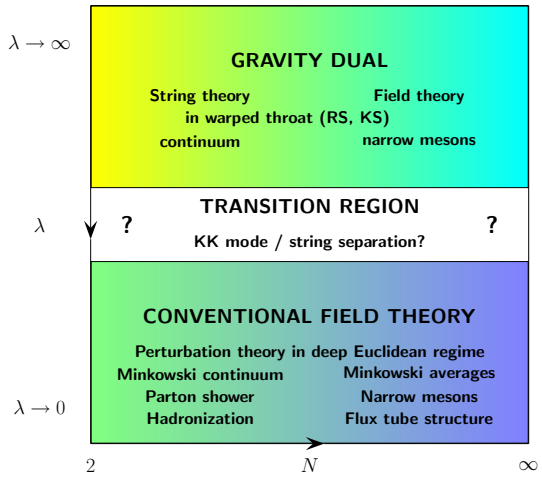

Figure 1: A survey of the $N - \lambda$ plane.

gravity dual). On the other hand, for large λ we expect the existence of a weakly coupled gravity dual, which is generically a string theory; however for large N the string modes decouple and a pure gravity dual should be enough to describe the theory. Thus we get the basic characterization of the four corners of the (N, λ) plane: for large N, λ the theory is reminiscent of a Randall-Sundrum [9] (or Klebanov-Strassler [10]) model: field theory (and classical gravity) on a warped background. For large λ, small N one should find string theory on a warped background. For large N, small λ we still expect a stringy description, but not necessarily higher dimensional, while for small N, λ we get ordinary perturbative QCD, with its characteristic parton showers followed by hadronization.

The main aim of this paper is to examine the various transitions in the (N, λ) plane. At first sight changing N from small to large values looks like a very dramatic transition, since in the large N limit the decays of mesons will be $1/N$-suppressed. As a result, at strictly infinite N, the theory behaves vastly differently from a small N field theory. In infinite N QCD, an e^+e^- collider would produce no hadrons at all, except when tuned to have *precisely* the energy of a resonance. However at small enough N, above the first few resonances, the spectral function will be dominated by a smooth, flat continuum. This is true at any λ: the cross section at small N is continuum, but at large N is a discretuum. At very large but finite N, we can study production of narrow on-shell mesons which subsequently decay. In the large-λ case these mesons are KK modes. In the small-λ case, they are flux tubes.

Arguments for the flux tube description of hadrons date back to the 1970s, and include in particular 't Hooft's characterization of phases of gauge theories based on the behavior of Wilson and 't Hooft operators [11]. Roughly speaking, there is a discrete set of possibilities for these behaviors, one of which is the confining area-law behavior of the Wilson loop, which suggests that the partition function has contributions of the form $e^{-\Lambda^2 LT}$. This suggests that there are states in the theory with constant energy density per unit length, so that their energy is $E = \Lambda^2 L$. Such states would look stringy. Various aspects of this argument have

been made with various amounts of precision over many years; a partial list of references can be found in Ref. [12]. The upshot is that confinement, in the sense of area-law behavior over some range of distances, implies that hadrons are approximately described by the Nambu-Goto action. There are similar flux tube states at large 't Hooft coupling [13, 14], but they are parametrically heavier, and we will not discuss them here.

Our goal in this paper is to argue that the small N to large N transition, at given λ, is fairly smooth and does not drastically alter qualitative properties of the physics, despite the singular nature of the infinite N limit; in other words, we expect to have a significant overlap between partonic, QCD-like descriptions, and hadronic, narrow-resonance descriptions. This supports the picture of "parton-hadron duality." On the other hand, the transition from small to large λ is in some ways more mysterious. Large 't Hooft coupling produces deeply bound meson (and glueball) states that do not resemble the experimentally observed mesons (in particular, they do not fall on linear Regge trajectories), but which are calculable in supergravity duals [15–20]. The exotic properties of light, low-spin states at large 't Hooft coupling have been emphasized in Refs. [4,17,18]. Certain decay modes and form factors are strongly suppressed at large 't Hooft coupling [18, 21]. Other aspects of the large 't Hooft coupling physics have been studied that contribute to the picture that strong coupling at short distances leads to novel physics [22–24]. The most recent such observation is that, whereas small λ leads to the familiar jet structure in QCD-like events, large λ leads to very spherical events as proved by Hofman and Maldacena. As far as we are aware, there is no tool currently available that can tell us whether the spectrum and event shapes transition smoothly as a function of λ or change abruptly at some critical λ. The latter possibility may seem strange, but a similar transition happens in the spectrum of modes of a static flux tube in $\mathcal{N} = 4$ SUSY Yang-Mills [25]. At large λ many issues involving very high energy scattering of hadrons, such as Regge trajectories, the Pomeron, and saturation [4, 26, 27], have been studied. Despite substantial quantitative differences, and some qualitative ones (e.g. the Pomeron couples to individual partons at small λ, but to hadrons at large λ), many aspects of the physics of high energy scattering (e.g. the saturation of the Froissart bound) are similar at small and large λ. Nonetheless, the details of dynamical questions at energies near the scale of the lightest resonances are strikingly different at small and large λ.[1] We should emphasize that this idea occurs, in various forms, throughout the literature, and is not new to us. However, we hope to present particularly simple and clear illustrations of the different regimes and make it apparent that these differences are generic, not artifacts of particular examples that have been studied in the past.

The paper is organized as follows: in section 2 we study the connections between the predictions of perturbation theory (PT) for a two-point function of currents, $\langle J(x)J(0)\rangle$, and the large N spectrum. At any λ, the deep Euclidean behavior of such a two-point function is determined by conformal symmetry, and unitarity relates the Minkowski and Euclidean limits. Various possible spectra are consistent with these two facts. However, in the perturbative case, we expect the leading-order deep Euclidean calculation to capture the physics almost everywhere in the complex plane, with small corrections. We confirm

[1] Another argument against the existence of a gravity dual of QCD was recently made in [28].

this expectation by showing that a large-N Regge-type spectrum, $m_n^2 \sim n$, is consistent with PT in most of the complex plane, except very near the Minkowski axis. At finite N the poles become cuts, but the behavior of the two-point function in most of the complex plane will be similar. On the other hand, the RS-type spectrum, $m_n \sim n$, deviates sharply from PT in much of the complex plane. There is nothing wrong with this, but it implies we should only expect such a spectrum in theories with large 't Hooft coupling, where PT breaks down very badly. The analysis of the spectrum continues in Section 3, which presents a simple quantum-mechanical toy model that illustrates how the spectrum of light states can change continuously from flux tube-type to RS-type as a coupling constant is varied. This suggests that the KK-like modes that are characteristic to AdS/QCD are actually not QCD states, but rather they are deeply bound mesons, that are more related to the short-distance Coulomb-like potential, and not to the long-distance confining linear potential.

Having established the large-N spectrum looks quite different at large and small λ, we turn our attention to more detailed properties of scattering events. We look at large but finite N, so that we can produce a narrow resonance on-shell and watch it decay in a sequence of steps. First we examine decays of Kaluza-Klein modes in an extra dimension in section 4. We show that the end result of the decay chain is a large number of the lightest modes moving in approximately independent directions, so that events appear spherical. We repeat the analysis for a soft-wall type background, and show that the spherical nature of the event shapes remains. Although we cannot reliably calculate the same process at small N, where stringy corrections would be important, we note that the physics is similar to that computed by Hofman and Maldacena, in which conformal theories at large N and λ give rise to spherical events. We speculate that large sphericities are characteristic of any large λ theory.

In section 5, we repeat this analysis for a different model of hadrons, namely quasi-stable flux tubes as we would expect to find in small λ, large N theories. We study models of flux tube evolution and breaking (motivated by Schwinger pair-production in the chromoelectric field), and find that the resulting events have a characteristic "jetty" structure, with energetic particles moving in opposite directions and only relatively soft particles in between. This is very similar to the well-known jet structure that arises from perturbative QCD and the parton shower, independently of any assumptions about hadronization. We take this as evidence that the small-N/large-N transition at small λ is much smoother than the small to large λ transition at large N.

These pieces of evidence, taken together, provide support for our picture of the (N, λ) plane. The old idea of parton-hadron duality is plausibly true everywhere in that plane, with the main effect of varying N being to broaden mesons until they merge with a continuum, with a large region of overlap between partonic and hadronic descriptions. The effects of raising λ are much more dramatic, with the spectrum of light excitations and the shape of events in a detector being starkly different in the small and large λ limits. We have no information about what the transition region is like; it may be smooth, with no phase transition, but it is at least a crossover between very different regimes. This suggests that if AdS/QCD is ever to be useful for truly QCD-like theories, we will need qualitatively new ideas and a better understanding of this transition region.

2 Perturbation Theory and the Large-N Spectrum

We are interested in understanding qualitative properties of confining gauge theories in the plane of the number of colors N and the 't Hooft coupling λ. Because we are interested in qualitative properties, we won't concern ourselves too much with which theory we are working in. In particular, for QCD it does not make sense to take λ very large, unless one considers a brane construction of a QCD-like theory with new degrees of freedom as in Ref. [29]. For concreteness, one could imagine studying the $\mathcal{N} = 1^*$ theory obtained by mass deformation of $\mathcal{N} = 4$ super-Yang-Mills, which has confining vacua in which one can vary N and λ [30,31]. In any case, we never have a fully controlled calculation over the whole plane, so we will have to pick certain corners and study them. In this paper we will be content with simplified calculations that exhibit general qualitative properties of the corners of the (N, λ) plane that we are interested in.

In a theory with small 't Hooft coupling at short distances, we can do a reliable perturbative calculation of the two-point function of a current in the deep Euclidean region. We trust from the operator product expansion that corrections to the calculated behavior are controlled: they are either proportional to a small coupling, or they are power-suppressed. The total cross section of a process like $e^+e^- \to$ hadrons is computed by analytically continuing the Euclidean answer to the Minkowski region and taking the discontinuity across a cut. At large N, we know that the cross section vanishes except exactly on a resonance. This tells us that the large-N behavior of the two-point function is controlled by a meromorphic function, i.e. one which is analytic throughout the complex plane except at a discrete (but infinite) set of poles. It turns out that there are different meromorphic functions that have the same deep Euclidean asymptotics. However, we will argue that some of these meromorphic functions are much closer to the perturbative answer over the whole complex plane than the AdS/QCD-like meromorphic function, so already PT for the two-point function seems to be telling us something important about the spectrum of hadrons.

Two decades before AdS/CFT or any examples of confinement with large 't Hooft coupling at short distances, Migdal attempted to find a large N ansatz for the QCD spectrum by Padé approximation of perturbative Euclidean calculations [32]. The idea behind the Padé approximation is to produce an analytic continuation of the perturbative result for $\Pi(Q^2)$ into the non-perturbative regime. The leading order perturbative result for the two-point function of two conserved currents is just given by (dropping a factor of $\frac{N}{12\pi^2}$ for convenience)

$$\Pi_{PT}(s) = \log \frac{s}{\mu^2} + \mathcal{O}\left(\frac{1}{s^2}\right), \tag{2.1}$$

with $s = Q^2$. In the Padé approximation one is looking for a ratio of two polynomials $\Pi_P(s) = P_N(s)/Q_N(s)$ which at a given point (for example $s = 1$) reproduces the first $2N + 1$ terms in the Taylor series of Π_{PT}. One can then take a limit as the order of these polynomials increases, finding a function with infinitely many poles. The resulting function obtained this way for $N \to \infty$ is

$$\Pi_P(s) = \frac{J_0(\sqrt{-s/\beta}) \log(-s/\beta) - \pi Y_0(\sqrt{-s/\beta})}{J_0(\sqrt{-s/\beta})}. \tag{2.2}$$

Here β is chosen as $(2x_1^2)^{-1}$ where x_1 is the smallest root of $J_0(x)$; this is chosen such that $\Pi_P(s)$ has its first pole at $s = 1/2$. We can see in Fig. 2 that it is a very good approximation to the PT result for large Euclidean momenta (by construction).

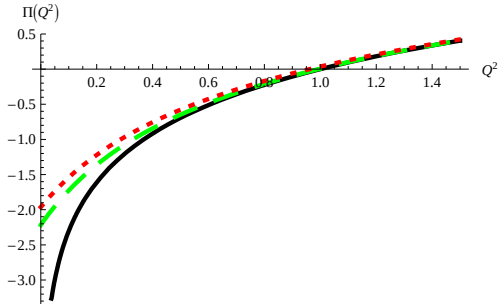

Figure 2: Perturbation theory vs. meromorphization at Euclidean momentum, $\Pi(Q^2)$: black solid line, $\log Q^2$; green dashed line, Padé approximation; red dotted line, digamma function.

It is well-known that this Padé approximation fails to capture some of the essential features of the non-perturbative physics of QCD. For example, the poles of Eq. (2.2) appear at $m_n^2 \sim n^2$, in stark contrast with the expected Regge answer $m_n^2 \sim n$. The difference between two-point functions with these types of behavior in the Minkowski region is illustrated in Figure 3. While Migdal's answer does not match the expected QCD-like behavior, it is remarkably precisely what one would calculate in the AdS/QCD framework [2], which can be considered as a simple model of what this quantity would look like in a theory at large 't Hooft coupling. This correspondence was first pointed out by Shifman in Ref. [33], and has been further discussed in Refs. [34]. Thus, while Migdal failed to produce a good model of the QCD two-point function, he stumbled upon a good model of large 't Hooft coupling theories!

As a contrasting model, one could consider the digamma function, $\psi(x)$, which is the logarithmic derivative of the gamma function,

$$\psi(x) = \frac{\Gamma'(x)}{\Gamma(x)} = -\gamma + \sum_{k=0}^{\infty}\left(\frac{1}{k+1} - \frac{1}{x+k}\right). \tag{2.3}$$

This function has the asymptotic expansion:

$$\psi(x+1) \approx \log(x) + \frac{1}{2x} - \sum_{n=1}^{\infty}\frac{B_{2n}}{2nx^{2n}}, \tag{2.4}$$

so that it has the right sort of behavior to match perturbative asymptotics. This function has been discussed as a model of a QCD-like spectral function a number of times in the literature, beginning with Ref. [35]. It allows us to build a model of the spectral function with the first pole in the same location (setting the ρ mass), $s = 1/2$, as:

$$\Pi_R(s) = \psi\left(s - \frac{1}{2}\right). \tag{2.5}$$

Note that this function, unlike the Padé result, has poles evenly spaced in m^2, not in m, so that it matches expectations for QCD. We show this function in the plots for comparison.

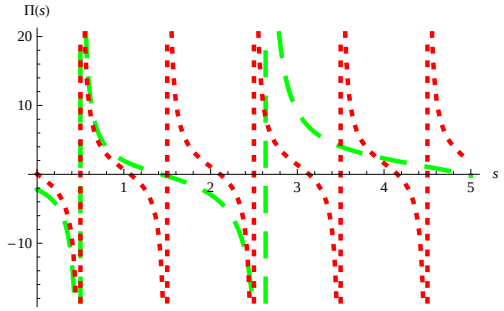

Figure 3: Different mass spectra with similar deep Euclidean asymptotics for $\Pi(s)$: green dashed line, analytic continuation of the Padé approximation; red dotted line, digamma function.

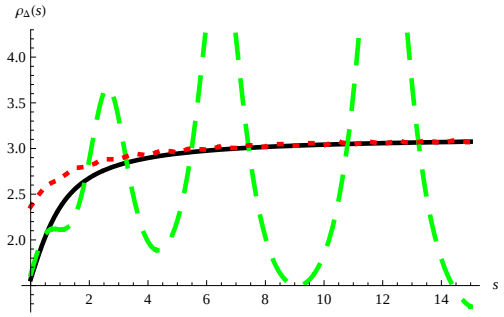

Figure 4: Smeared spectral function, $\frac{1}{2i}(\Pi(s+i)-\Pi(s-i))$: black solid line, perturbation theory; green dashed line, Padé approximation; red dotted line, digamma function. The digamma function with proper Regge physics provides a reasonably good match, while the Padé approximation oscillates about the perturbative result with large amplitude.

The obvious question is which of these approximations one should take more seriously for the case of large N and small 't Hooft coupling. On the face of it both of these functions reproduce the perturbation theory results quite precisely. However, we will argue that that despite the good agreement with PT for the deep Euclidean region the Padé approximation actually does not match PT over the whole complex plane all that well, and that other functions like $\Pi_R(s)$ exist that will capture the global features of PT much better. To understand why the Padé approximation fails we need to understand the region of momenta where the Padé approximation is bad. Clearly it is doing extremely well for the deep Euclidean region. However, some of the Minkowski region should also be attainable through PT, at least when we are away from the poles, i.e. away from the real axis $s > 0$. One particularly simple

quantity of this sort is a smeared version of the spectral function ρ:

$$\rho_\Delta(s) = \frac{1}{2i}\left(\Pi(s+i\Delta) - \Pi(s-i\Delta)\right). \tag{2.6}$$

A function of this sort has been discussed by Poggio, Quinn, and Weinberg [36]. Many comparisons of experimental data on QCD with PT implicitly rely on an approximate *local* quark-hadron duality that allows a result smeared over hadronic resonances to match PT. At low orders of PT, the choice $\Delta \sim 1$ is effectively an infrared cutoff at about the scale Λ_{QCD}. (In fact, since $s = 1/2$ here corresponds to the ρ mass squared, this acts like an IR cutoff of about 1 GeV.) However, the Padé approximant disagrees quite sharply with the expected PT answer, as can be seen in fig. 4. It would be rather surprising if such a smeared perturbative calculation could disagree so strongly with the true hadronic answer at large values of Minkowski momentum! On the other hand, the smeared spectral function calculated from the digamma function Π_R will still be a very good approximation to the PT answer even for Minkowski momenta. The agreement is shown over the complex plane in Figure 5. Note that Π_R has larger error in a Λ_{QCD}-size region around the origin, but otherwise disagrees only in a narrow strip along the Minkowski axis. (Of course, one should not expect that the agreement is good until $|Q^2| \gg \Lambda_{QCD}$, so this is entirely as expected!) On the other hand, the Padé result Π_P has large error in a wedge that grows progressively larger as one goes deeper into the Minkowski region.

One would hope that one could complete Migdal's program of uniquely fixing the appropriate meromorphic function relevant for large N QCD by also requiring a good match to the Minkowski region. An attempt in this direction is described in detail in Appendix A, where we do show that the spacing between the poles $m_{n+1}^2 - m_n^2$ should not be growing, and that the simplest meromorphic function satisfying all constraints from PT has asymptotic properties agreeing with those of the digamma function. However, we could not exclude some more exotic possibilities, so we conclude that Migdal's hope of finding a systematic procedure to convert perturbative results to meromorphic functions does not seem tractable, at least when only the two-point function is considered.

To summarize this section: we found that in order to apply Migdal's program of analytically continuing the perturbative result one should use the digamma function rather than the Padé approximation. The use of such meromorphic functions with QCD-like spectra has been previously discussed; see, e.g., Refs. [35, 37]. The result obtained by Padé approximation is a good guide to the large 't Hooft coupling spectrum (that is the case when AdS is a good description). Of course, at large 't Hooft coupling PT breaks down, so it should not be surprising to see that there can be a qualitatively different spectrum for a large 't Hooft coupling. In the next section we will discuss a very simple toy model that illustrates how the spectrum can change as the 't Hooft coupling changes.

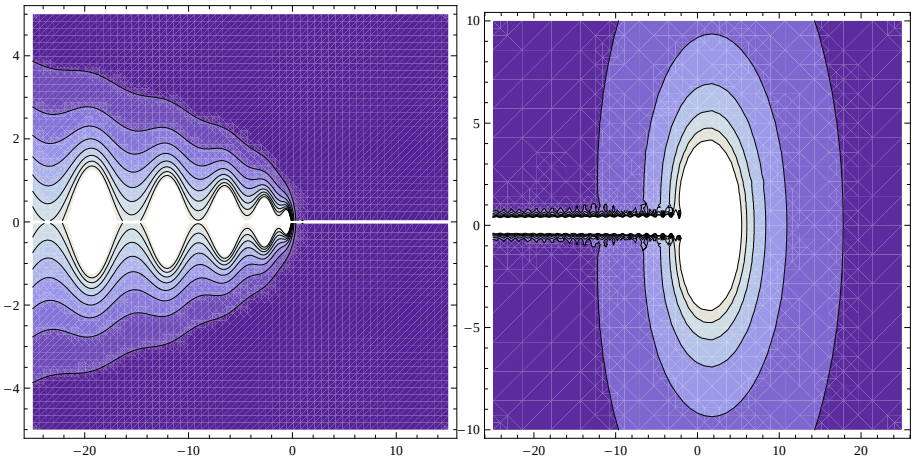

Figure 5: Contours of constant fractional difference, $\frac{\Pi(q^2)-\log(q^2)}{\log(q^2)}$, between the leading-order perturbative result and the full two-point function. At left is the Padé case Π_P and at right the digamma function Π_R. White regions correspond to large fractional disagreements, and dark regions to very good agreement. The digamma function disagrees with PT in a circle of order Λ_{QCD}, and very close to the Minkowski axis, while the Padé approximant disagrees in a growing wedge in the Minkowski region.

3 A toy model of bound states: where have all the KK modes gone?

We have seen that a QCD-like spectrum is much more consistent with perturbative calculations than a Padé or AdS/QCD-like spectrum. It would be interesting to understand in more detail how the spectrum can change as one varies the 't Hooft coupling. In this section we will discuss a very simple toy quantum-mechanical model of bound states in which the spectrum can change between QCD-like and AdS/QCD-like. We make no claim that this is an accurate model of the dynamics of any quantum field theory, but it does provide some intuition about how strong coupling at short distances can change the spectrum.

For studying the spectrum of mesons in a QCD-like theory, we expect that we have a confinement potential well-approximated by the Cornell form,

$$V(r) = -\frac{\lambda}{r} + \sigma r, \tag{3.1}$$

with σ the string tension. The spectrum of mesons is, at least qualitatively, determined by a relativistic bound-state calculation involving this sort of potential. (There have been various studies of meson and glueball spectra in Coulomb gauge QCD, which resemble these potential models, including some which are quite sophisticated [38].)

What is notable about the large λ examples is that the non-QCD-like states have masses of order M where $M \sim \lambda^{-1/4}\sqrt{\sigma} \ll \sqrt{\sigma}$. This suggests that these bound states involve physics at distances where the σr term of the potential is not yet dominant. Rather these

states seem to be related to the short-distance part of the potential, and so they are likely better characterized as deeply bound mesons due to the Coulomb nature of the potential at short distances. In QCD, there is only one scale, Λ_{QCD}, and it's difficult to see how such states could arise. So let's turn our attention away from QCD and instead think about $\mathcal{N} = 4$ super-Yang-Mills deformed by mass terms to an $\mathcal{N} = 1$ confining theory. The mass terms give one scale, m, at which we expect strongly-bound mesons at large λ, where the string tension is $\sqrt{\lambda}m^2$.

The static potential is computed along the lines discussed by [39]. In particular for RS (as discussed in [41]) it will be Coulomb-like until the string is long enough to reach the IR brane; at that point, any additional string length lies along the IR brane and the potential grows linearly. In other words,

$$V(r) = \begin{cases} -\frac{c}{r}, & r \leq r_c \\ -\frac{c}{r_c} + \sigma(r - r_c), & r \geq r_c \end{cases} \tag{3.2}$$

Here

$$c = \frac{4\pi^2 \left(2g_{YM}^2 N\right)^{1/2}}{\Gamma\left(\frac{1}{4}\right)^4} \approx 0.3231\sqrt{\lambda}, \tag{3.3}$$

as in the AdS/CFT calculation. We can read off from Maldacena's calculation of the static quark-antiquark potential that the string just touches the IR brane at z_{IR} when the quark and antiquark are separated by a distance

$$r_c = z_{IR}\frac{(2\pi)^{3/2}}{\Gamma\left(\frac{1}{4}\right)^2} \approx 1.198 z_{IR}. \tag{3.4}$$

Finally, the string tension is given in terms of the 't Hooft coupling and the location of the IR brane:

$$\sigma = \frac{1}{2\pi\alpha'}\frac{R^2}{z_{IR}^2} = \frac{\sqrt{\lambda}}{2\pi z_{IR}^2}. \tag{3.5}$$

Our approach will be to use this potential to model the confining force between a scalar quark and anti-quark in a simple toy model of relativistic quantum mechanics. That is, we solve for radial excitations that are eigenstates of the Hamiltonian

$$H = \sqrt{p_r^2 + m^2} + V(r), \tag{3.6}$$

where p_r is the radial component of the momentum. One can think of this as a very rough approximation to a Hamiltonian formalism for the theory in Coulomb gauge, approximating the Coulomb potential by the Wilson-loop potential, although strictly speaking they are known to differ [40].

We will make one further approximation in order to do more of the problem analytically, which facilitates an easy numerical solution for the eigenstates. Namely, we will use a variational ansatz with basis functions of the form $e^{-\beta r}L_n^2(2\beta r)$, and we would like a potential

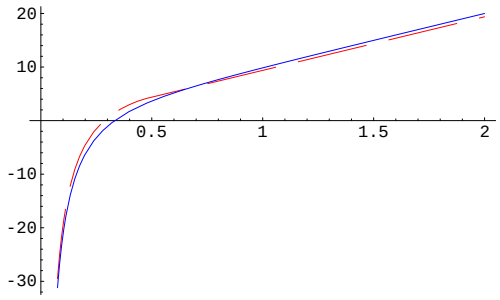

Figure 6: Comparison of the RS potential (red, dashed), shifted by a constant value of 10.5, and our analytically useful replacement of it (blue, solid).

$V(r)$ that has analytically calculable overlap with these basis functions. In particular we take the parameters of the model to be specified by $m = 1$, $\sigma = 10$, $c = 3$ (note that with these parameters $\sqrt{\lambda} \approx 9.28$ is large), and we approximate $V(r)$ by the more analytically tractable:

$$V_{mod}(r) = -\frac{3}{r}\exp(-3r) + 10r, \tag{3.7}$$

in effect changing the sudden θ-function like cutoff to a smoother exponential shut-off of the Coulomb part of the potential.

This modified potential agrees quite well with the original RS potential, shifted by a constant value of 10.5, as illustrated in Figure 6. Because there is no clear correct definition of the zero of the potential, we will ignore the constant shift. (Of course, if we look for evenly spaced masses, a constant shift in energy eigenvalues is irrelevant; if we look for evenly spaced *squared* masses, a constant shift will matter, but will become less important at high enough excitation number.)

Finally, to get a toy model of the transition from a QCD-like spectrum to an RS-like one, we vary the coefficient of the first term in $V_{mod}(r)$:

$$V_\gamma(r) = -\frac{\gamma}{r}\exp(-3r) + 10r. \tag{3.8}$$

At $\gamma = 0$ we have only a linear term, resembling a QCD-like theory where Coulomb attraction plays very little role in the pattern of bound states, while at $\gamma = 3$ we have a theory which more closely resembles RS. The squares of the eigenvalues of the Hamiltonian $\sqrt{p_r^2 + m^2} + V_\gamma(r)$ are plotted for $\gamma = 0, 1, 2, 3$ in Figure 7. One can see that as the strong Coulomb attraction is turned on, the low eigenvalues become closely spaced and take on a qualitatively new character (although they change continuously). These are deeply bound states, sensitive to the strong short-distance Coulomb attraction and relatively insensitive to the long-distance linear confinement. They are the toy model analogs of KK modes. Higher eigenvalues are spaced successively farther apart, eventually merging into the original pattern of linearly spaced mass-squared. They are the toy model analogs of resonances

on linear Regge trajectories. Note that at $\gamma = 0$ one finds roughly even spacing consistent with $m^2(n+1) - m^2(n) = \frac{1}{\alpha'}$.

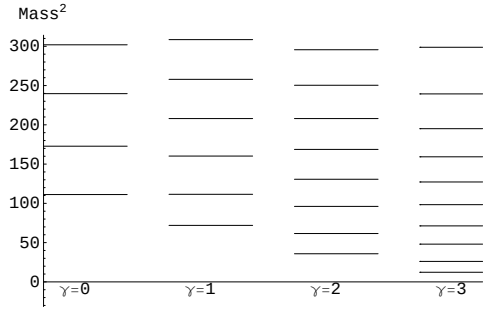

Figure 7: Spectrum of our toy Hamiltonian .

A more reliable and field-theoretic approach to modeling the effect of strong short-distance Coulomb attraction on bound states would be to use Bethe-Salpeter equations, but already our toy model has interesting physics that suggest a picture of how the transition from QCD-like to RS-like dynamics can happen. As a final remark on this topic, we should point out that literature beginning from a "soft wall metric" background [42] computes AdS/QCD potentials which are good matches to lattice data and which work well phenomenologically in Salpeter calculations [43]. On the other hand, we will see in the next section that event shapes in soft wall backgrounds are not QCD-like, so if such potentials are to fit into a coherent framework for QCD phenomenology, one would have to understand stringy corrections to the effective action.

4 Dynamics for large N, large λ: Spherical Event Shapes

So far we have been discussing the two-point function of a current with itself, which determines the spectrum of associated resonances and the total cross section of a process like $e^+e^- \to$ hadrons. However, the real physics of $e^+e^- \to$ hadrons is much richer: in QCD, for instance, we know that such an event will lead to a parton shower that produces collimated jets of particles moving in a small number of directions. We now want to turn our attention away from the crude questions of spectrum and cross section and toward the richer questions about the structure of events. This will mean going to finite N and considering how resonances decay and broaden into continuum structure.

Our tool for understanding whether an event is spherical or jetty will be the "sphericity" [44], which is defined as $S = \frac{3}{2}(\lambda_2 + \lambda_3)$ where λ_2 and λ_3 are the two smallest eigenvalues of the matrix:

$$S_{jk} = \frac{\sum_i p_j^{(i)} p_k^{(i)}}{\sum_i \left|\vec{p}^{(i)}\right|^2}, \tag{4.1}$$

where $p^{(i)}$ is the 3-momentum of the i^{th} final-state particle. The sphericity is 1 for a completely spherical event, and 0 for two back-to-back particles. Perturbative QCD predicts small sphericities of order few$\times 0.01$.

Extra dimensions, in general, predict a sizable sphericity. To see why, recall that in a flat periodic extra dimension, or a flat interval with Neumann boundary conditions on both ends, there is a discrete conserved 5D momentum, or "KK number." The wave functions are cosines and triple overlaps vanish except when the mass of the highest state is precisely the sum of the masses of the two lower states. This case is not very interesting; there is no phase space for decays. In a UED model, the exact KK number conservation is broken by boundary masses or by localized boundary kinetic terms. However, in this case, as in many other theories with an extra dimension, there is still an approximately conserved KK number. In particular, in a two-body decay of a heavy KK mode, the masses of the two daughters are very close to being equal to the mass of the parent; as a result, there is little phase-space and the daughters are not very boosted. Thus, if they subsequently decay, the new daughters will again not have much of a boost, and the momenta of the various particles in the final state will not be strongly correlated with any particular direction. This leads to spherical events.

In particular, Figure 8 shows one example of the shape of such an event. This is the decay of a heavy KK mode of a gauge boson in flat space with a Neumann boundary condition on one end of the space and a Dirichlet boundary condition on the other. The spikes radiated out represent the momenta of stable daughters at the end of the decay chain, with length proportional to energy. Note that daughters are flying out in all directions, and if we were to place a spherical detector of large radius around the origin, it would see a fairly uniform distribution of energy. In particular, the sphericity is high. This is not a jetty event, but one closer to the uniform energy distribution found in the conformal case [5]. The distribution of sphericity for such decays is also shown in Figure 8, where we see that an overwhelming fraction of events have fairly large sphericities > 0.1.

Although approximate conservation of KK number is most obvious in flat space, it turns out that even in warped space it is still true. As a first example we consider a scalar field in an RS background with cubic interaction:

$$S = \int d^4x \int_{z_{UV}}^{z_{IR}} dz \left\{ \left(\frac{R}{z}\right)^3 (\eta^{\mu\nu}\partial_\mu\phi\partial_\nu\phi - \partial_z\phi\partial_z\phi) + \left(\frac{R}{z}\right)^5 g_5\phi^3 \right\}, \tag{4.2}$$

with R the AdS curvature radius. We take $z_{UV} \to 0$, requiring that wave functions be normalizable at the boundary, and we impose a finite z_{IR} where Dirichlet boundary conditions are imposed. This means that our wave functions are:

$$\psi_n(z) = \frac{z^2 J_2(m_n z)}{\sqrt{-R^3 z_{IR}^2 J_1(m_n z_{IR}) J_3(m_n z_{IR})/2}}, \tag{4.3}$$

where $J_2(m_n z_{IR}) = 0$ and the denominator serves to normalize the wave function.

From these wave functions, we can compute couplings as triple overlaps and then compute decay chains. While it is not obvious from inspecting the wave function, it turns out that

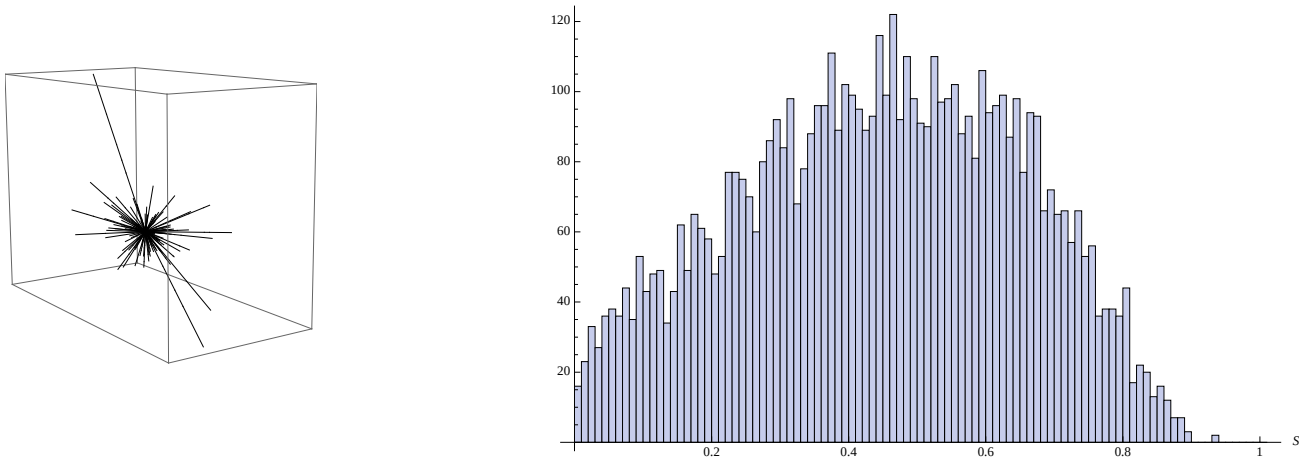

Figure 8: On the left: typical spherical event from the decay of the 200th gauge KK mode in flat space. On the right: the sphericity distribution from 6000 decays of the 200th gauge KK mode in flat space.

the triple overlaps still show a strong tendency to almost conserve KK number, so that decays with little phase space are preferred. As an illustration of this, we plot in Figure 9 the distribution of the speeds, $v_{1,2} = |\vec{p}_{1,2}|/E_{1,2}$, of the two KK modes originating from the decay of the 100th scalar KK mode in RS. Notice that in almost every case, the decay is to two relatively slow-moving, unboosted particles; the masses of the two daughters sum to nearly the mass of the parent. Just as in flat space, the tendency to prefer decays with little

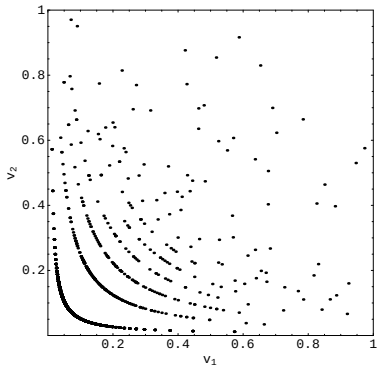

Figure 9: Distribution of the speeds v_1 and v_2 of the two Kaluza-Klein modes originating from the decay of the 100th scalar KK mode in RS. Note that typically the decay is to slow-moving particles.

phase space will lead to very spherical events. A typical such event for the decay of a heavy gauge KK mode in RS is shown on the left panel in Figure 10, and the sphericity distribution for many such events is shown in the right panel in Figure 10. Because the zeroes of Bessel functions are very nearly linearly spaced, it turns out that the number of the KK mode is

almost conserved. This is illustrated in Figure 11. The 200th KK mode decays most often to two modes with mode number summing to 198, then to 199, then to 197, and so on.

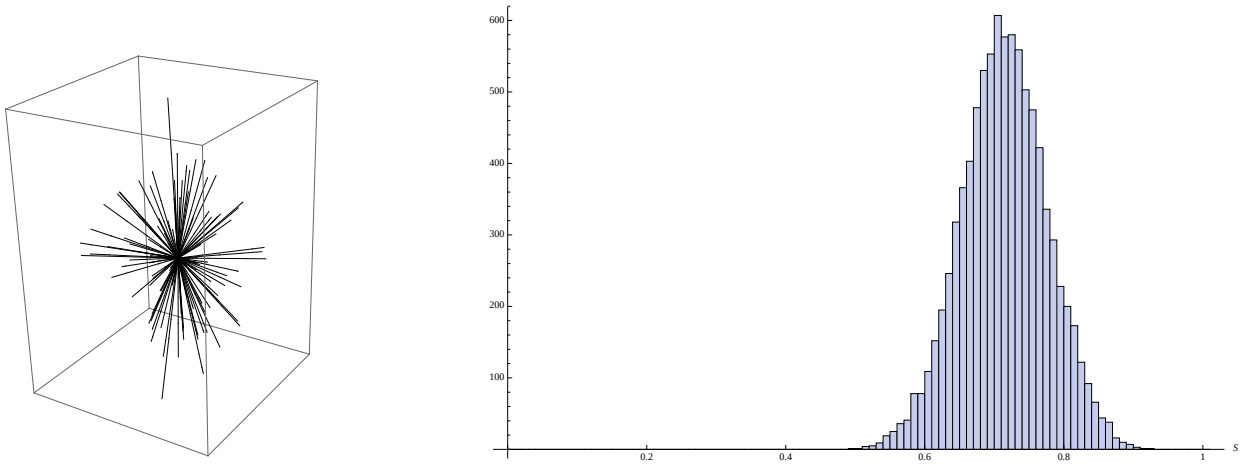

Figure 10: Left: a typical spherical event from the decay of the 200th KK gauge KK mode in AdS. Right: Sphericity distribution event from 9000 decays of the 200th gauge KK mode in AdS space.

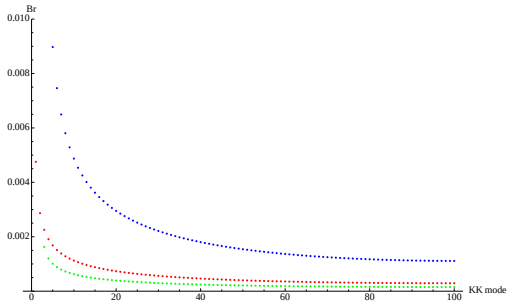

Figure 11: Branching fractions for the 200th KK mode with the KK number of one of the daughters on the horizontal axis. In the top line (Blue) the KK numbers of the daughters add up to 198, in the second line (Red) they add to 199, in the third line (Green) they add to 197.

RS backgrounds are similar to flat space, to the extent that they predict mass spectra with nearly linear spacing. What happens if we tune an extra-dimensional theory to achieve the Regge spacing $m_n^2 \sim n$, which holds in small 't Hooft coupling theories as discussed in the previous sections? One might hope that almost-conservation of KK number is lost and event shapes are very different. We will now see that is not the case; despite the very different spectrum, decays with little phase space are still preferred and sphericities are large. Our starting point will be a gauge field in the by now familiar "soft-wall" model of AdS/QCD,

in which the metric is AdS but the action is [45]:

$$S = \int d^5x\ e^{-\Phi}\sqrt{g}\frac{-1}{4g_5^2}F_{MN}F^{MN}, \tag{4.4}$$

$$e^{-\Phi} = e^{-\Lambda^2 z^2}. \tag{4.5}$$

The exponentially damped dilaton leads to an equation of motion that can be rewritten as a Schrödinger equation for the eigenvalues m_n^2 with harmonic oscillator potential $\sim z^2$ at large z, which yields the desired spectrum. In the original soft-wall model, the dilaton is simply assumed to have this profile, due to some unknown dynamics.

In this model, triple overlaps of wave functions vanish; we must deform it slightly to get a model in which we can calculate decays. As a simple deformation, we include a "UV brane" at $z = z_{UV}$ and impose Dirichlet boundary conditions there (the other boundary condition is simply normalizability at $z \to \infty$). This gives a small deformation to the wave functions and masses and allows us to compute decay chains. It turns out that the correct wave functions are given by:

$$\psi_n(z) = c_n z^2 U\left(\frac{-m_n^2}{4\Lambda^2} + 1, 2, z^2\right), \tag{4.6}$$

with U a confluent hypergeometric function. The condition $U\left(\frac{-m_n^2}{4\Lambda^2} + 1, 2, z_{UV}^2\right) = 0$ determines the masses m_n and the constant c_n is chosen to give canonically normalized KK modes.

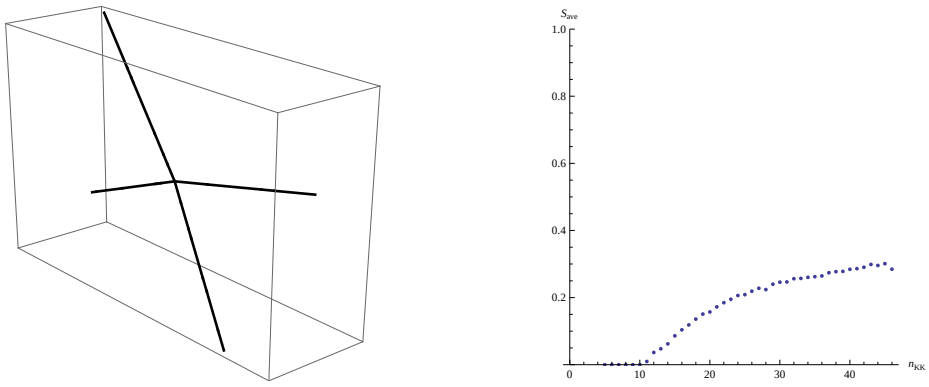

Figure 12: At left: a typical spherical event from the decay of a heavy (the 46th mode) soft-wall gauge boson. The UV brane was chosen to be at $z_{UV} = 0.01/\Lambda_{QCD}$. At right: average sphericity in 500 decays of the nth KK gauge boson in the soft-wall background. The horizontal axis is the KK number and the vertical the average spehricity of 500 decays of that mode.

In Figure 12 we show a typical spherical event, and the distribution of sphericities. The numerical treatment of the hypergeometric U-function is much harder than that of Bessel functions, and due to the smaller spacing among the masses there are fewer kinematically

allowed decays for a given KK mode. Nevertheless, even with a relatively low number of events the trend toward final states with larger sphericities is quite clear. This is again because despite the very different mass spectrum, the wavefunction overlaps prefer the decays with small phase space and correspondingly small boosts. The soft wall predicts more spherical events which are un-QCD-like, despite its QCD-like mass spectrum. Attempts to put the soft-wall background on a dynamical footing, as in Ref. [46], seem unlikely to remedy this problem unless they involve inherently stringy dynamics. One perhaps more promising direction, begun in Ref. [47], is to begin with the solvable large-N 't Hooft model in 1+1 dimensions and attempt to reformulate it as a 2+1 dimensional theory. Such an approach could also clarify the relationship between holographic wavefunctions and the internal structure of hadrons [48]. It remains to be seen how far this program can be pushed, and whether it will lead to anything resembling the soft wall. Also, note that demanding "asymptotic freedom" in the sense of a 5D dilaton which approaches a weak coupling value will not change these event shapes. To truly model the dual of a weak coupling theory, one would have to include light fields (string modes) dual to the many operators with small anomalous dimension. For now, it seems that there is still a major obstacle to obtaining QCD-like dynamics from a 5D theory, one which will likely require new techniques in string theory to be overcome. For now, we will turn back to 4 dimensions, and look at how much older models of hadrons generate event shapes that are much closer to those of QCD.

5 Large N, Small 't Hooft Coupling: Flux tubes

5.1 Flux tube Breaking, Directionality, and Jets

If, as we have argued, the mesons of RS do not smoothly match onto the mesons of a QCD-like theory, what sort of mesons do? There is a long history of modeling the highly excited states of QCD-like theories using flux tubes. Among the reasons for doing this are the idea that large N QCD is a string theory because it has a topological expansion [8], the experimental fact of Regge trajectories [49], the emergence of flux tubes on the lattice [50], and general arguments about the behavior of 't Hooft versus Wilson loops [11, 12]. Unlike in theories with large 't Hooft coupling and good gravity duals, the stringy physics in confining theories at small 't Hooft coupling begins at the scale of the lightest resonances; there is no large $\sqrt{\lambda}$ to provide a parametric separation of scales.

Before we look at more detailed modeling of flux tubes, let's begin by thinking about the first breaking of the flux tube that would be produced, for example, in an e^+e^- collider. We begin with a quark and antiquark moving in opposite directions, each with momentum p, and assume they feel a linear potential, i.e. a constant attractive force σ toward each other. We assume the probability of breaking is uniform along the string length; thus, as the string grows linearly, initially the decay probability per unit time goes as t^2. If the string breaks immediately, then there are massless quarks moving in opposite directions, and we have a clean two-jet event, just as in PT. If the string breaks when fully extended, we have two heavy static flux tubes of mass $2px$ and $2p(1-x)$, with x the fractional distance along the

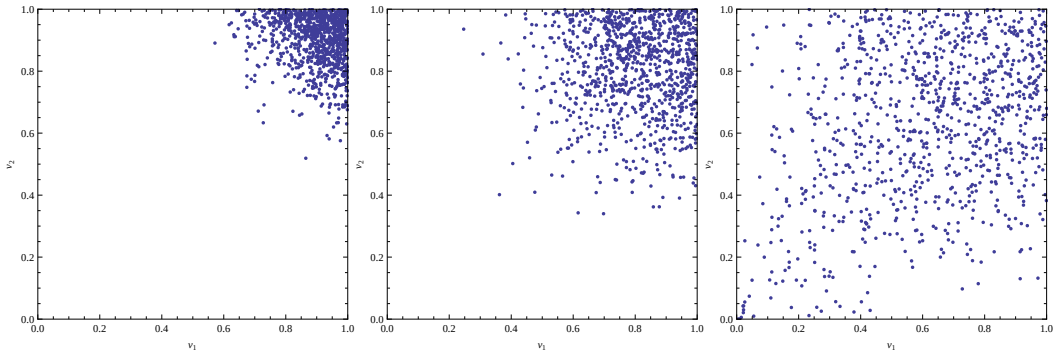

Figure 13: Distribution of the speeds v_1 and v_2 of the two flux tubes originating from breaking of an initial flux tube. The state begins with back-to-back quark and antiquark of 15 GeV momentum, and the string tension is 0.177 GeV^2. The decay rate per unit length is, from left to right, 0.01 GeV^2, 0.0025 GeV^2, and 0.000625 GeV^2. This corresponds to 99% of the strings having decayed by the time they are one-quarter, half, and fully extended, respectively. Note that even in the latter case many decays are to fast particles.

string where the break occurs. These flux tubes will subsequently decay, but the event will not be jetty. After the time $\tau_{osc} = p/\sigma$ at which the string is fully extended, the quark and antiquark turn around and again pick up speed, so at longer decay times there can still be many events at which the decay products are boosted.

In Figure 13 we show the distribution of speeds of the decay products as the decay rate decreases. Provided the string decays in a time smaller than that needed for the string to fully extend, the first breaking is to high-speed objects, and we expect that their further decays will widen the jets but maintain the qualitative "jettiness" of the event. The thrust axis of the jets will be the direction along which the flux tube was stretched, established by the initial momentum of the quark and antiquark, just as in PT. Note that in order for the string to decay before the quark and antiquark reverse direction, we need $\tau_{dec} < \tau_{osc}$. The decay time will be $\tau_{dec} \sim \frac{N}{p}$, so this tells us that we need N less than about $\frac{p^2}{\sigma}$. This is consistent with large N provided we look at strings that are energetic enough.

If the decay rate is sufficiently small, so that $\tau_{dec} > \tau_{osc}$, then we have slow daughters much more often, although the distribution is still very different than that for KK modes in Figure 9. Note, however, that for such small decay rates, the discreteness of the large N spectrum invalidates our way of thinking about the decay. Given $m_n^2 \approx n\Lambda^2$, we have

$$m_{n+1} - m_n \approx \frac{\Lambda}{2\sqrt{n}} \sim \frac{\sigma}{m_n}. \tag{5.1}$$

Thus the spacing between subsequent modes is of order the inverse of the oscillation time of our semiclassical string; if $\tau_{dec} > \tau_{osc}$, the width is smaller than the interval between subsequent modes, and it no longer makes sense to assume a continuous flux tube that can break at any location. In this situation a quantum mechanical treatment is required, and the resulting discreteness of the spectrum will play a role in calculating the decays. We are unable to treat such long decay times in the context of this semi-classical model.

5.2 A Simple Model of Flux Tubes

We have simulated a very simple toy model of the decay of an excited flux tube, in order to plot some event-shape distributions. The literature has many more elaborate models, with varying degrees of input from PT. Some early references are [51, 53–55]; more recently, the "gluon chain model" [56] has provided an example of a model that reflects both partonic and flux tube limits of the theory, and is consistent with important nonperturbative features of Yang-Mills theory like Casimir scaling at intermediate distances and N-ality scaling at long distances. (For a recent review of confinement in QCD-like theories, with an emphasis on the role of these features, see Ref. [57].)

Our model is a semiclassical one, based on linear confinement and decay by Schwinger pair production, following Ref. [51] as amended by Ref. [52] so that energy is conserved when the flux tube breaks. We begin with a quark and antiquark moving at high momentum in opposite directions along the z axis, separated by a constant chromoelectric field filling a cylinder of radius R, so that they are attracted by a constant force σ (the string tension). The total energy of the system is (taking the quarks to be massless):

$$E = \sum_q |\vec{p}_q| + \sum_{\bar{q}} |\vec{p}_{\bar{q}}| + \sum_{q\bar{q}} \sigma \, |\vec{x}_q - \vec{x}_{\bar{q}}| \,, \tag{5.2}$$

where the last term is a sum of the energy from string tension over quark–antiquark pairs. We do not reconnect pairs, so that each quark is associated with precisely one antiquark partner at all times (changing only when there is a decay). The flux tube can decay by the production of a quark-antiquark pair at some point along the axis between quark and antiquark. The newly created pair will have transverse momentum p_T (orthogonal to the flux tube axis) and the quark and antiquark will be separated by a distance $d(p_T) = 2E_T/\sigma$. The stretch of string that has been annihilated between the two quarks then compensates for the energy added by their initial momentum. Transverse momenta are distributed according to a Gaussian, $dN(p_T) \sim d^2p_T \ \exp\left(-\frac{\pi p_T^2}{\sigma}\right)$. Our simulation takes small time steps, alternating a classical evolution step and a random decay step. In the classical evolution step, quark-antiquark pairs evolve according to their current momenta and the color force between them, treating Eq. (5.2) as a Hamiltonian governing the evolution. (We never reconnect pairs, so each quark remains connected to the same antiquark until the string fragment splits, generating two shorter strings.) The random decay step decays each string fragment with probability proportional to the time step and to the length of the string fragment; decays happen with p_T (orthogonal to the quark-antiquark axis) chosen from the Gaussian distribution and location of the decay chosen from a uniform distribution on the string consistent with the newly produced pair having the correct separation $d(p_T)$ and remaining between the original quark and antiquark. This is a highly simplified model, neglecting for instance any internal dynamics of the string, but we expect it to get the grossest qualitative features right, at a level that allows an approximate comparison with the RS results and with QCD. It conserves energy (because the newly created pair are always separated by an appropriate distance along the string axis) and momentum (because the newly created pair have equal

and opposite momentum), but is not fully relativistically invariant[1]. In Section 5.3 we will discuss the relativistic string action and show that the first few decays computed from it are qualitatively consistent with the results of this simpler model.

For convenience we use the same string tension as in Ref. [51], $\sigma = 0.177$ GeV^2. We simulated a flux tube initially consisting of a quark and antiquark produced at the origin moving with $p_z = \pm 15$GeV along the z-axis. The overall decay probability is suppressed from the original calculations to take into account the effect of large N: for the plots shown the probability per unit time and unit length of a break is $\frac{p}{L\Delta T} = 0.01\text{GeV}^2$. We take time steps of 0.025 GeV^{-1}. As a stopping criterion, after each decay we flag as stable any new string segment that has

$$m = \sqrt{E(|\mathbf{x}_i - \mathbf{x}_{i+1}|, p_i, p_{i+1})^2 - |\mathbf{p}_i + \mathbf{p}_{i+1}|^2} < 1.54 \text{ GeV}. \tag{5.3}$$

As we can see in Fig. 14 these events are quite jetty, with very low characteristic sphericities, as expected in QCD.

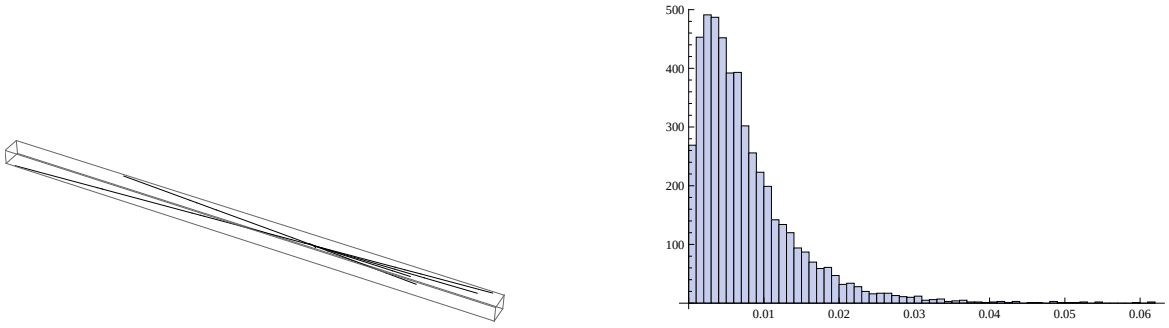

Figure 14: Left: a typical flux tube event from the decay of a 30 GeV flux tube in the toy model described in the text. Right: Sphericity distribution from 5000 decays of a 30 GeV flux tube in the toy model described in the text.

5.3 Including String Dynamics

We can move beyond this crude model of flux tubes by including stringy dynamics: we will model the flux tube worldsheet with the classical Nambu-Goto action. We specialize to static gauge, $t = \tau$, and parametrize the spatial coordinate s with the conditions

$$\partial_s \vec{X} \cdot \partial_\tau \vec{X} = 0, \tag{5.4}$$

$$\left(\partial_s \vec{X}\right)^2 + \left(\partial_\tau \vec{X}\right)^2 = 1, \tag{5.5}$$

which reduce the string action to

$$S_{NG} = \frac{\sigma}{2} \int d\tau ds \left(1 + \left(\partial_s \vec{X}\right)^2 - \left(\partial_\tau \vec{X}\right)^2\right), \tag{5.6}$$

[1]In Appendix B we show that for large enough center of mass energies it does give a Lorent invariant description.

so that the equations of motion are simple wave equations (for a detailed discussion, see the textbook [58]). Note that with this parametrization, the string energy is simply the tension σ times the length of the s interval.

There is a subtlety here: if we use just the Nambu-Goto action for the string, with Neumann boundary conditions, the string endpoints will always move orthogonal to the string direction. However, we begin with a string stretched along the z-axis between two quarks with momentum in the z-direction. The Nambu-Goto action alone will not suffice to describe this system. This puzzle is resolved by noting that the quarks on the ends of the string are physical particles, and we should add the action of a massive point particle at each string endpoint to the Nambu-Goto action, with the constraint that the string must end at the location of the point particle.[2] There is a recent discussion of this in Ref. [59] in the context of "quirks", hypothetical long strings of some new gauge group with $M_Q \gg \Lambda$, which we will follow for the key points. As in our simple Hamiltonian toy model, the quark (and antiquark) will experience a force, but now we can have a proper relativistic and local description: the force is related to the direction the quark moves in, and the direction tangent to the string at its endpoint. Specifically:

$$\vec{F} = -\sigma \left(\sqrt{1 - \vec{v}_\perp^2} \frac{\vec{v}_\parallel}{v_\parallel} + \frac{v_\parallel}{\sqrt{1 - \vec{v}_\perp^2}} \vec{v}_\perp \right), \tag{5.7}$$

where $v_\parallel$ is the component of quark velocity along the string direction and $\vec{v}_\perp$ is the orthogonal component. The corresponding rate of change of the quark energy is

$$\frac{dE_q}{dt} = -\sigma \frac{v_\parallel}{\sqrt{1 - \vec{v}_\perp^2}}. \tag{5.8}$$

If this force is acting to slow down the quark, then energy conservation will require that the quark leaves a new bit of flux tube in its wake. If the quark is speeding up, then it is eating some existing flux tube as it moves. Thus adding the point particle action at the string boundary is, from a certain point of view, an extreme deformation of the Nambu-Goto dynamics; we're not just studying a classical string that is moving relativistically, we're studying a string that grows and shrinks as it moves relativistically. As noted above, the static gauge parametrization that makes the string equation of motion simplest has the feature that the length of the s interval is the string energy in string units. To continue to use that parametrization in this context, we have to allow the size of the s interval to grow or shrink: if the string energy, in units of the tension, is $\varepsilon(t) = E_{string}(t)/\sigma$, then we can use a parametrization in which, for the initial back-to-back string, s takes values in

[2]Note that in the AdS/CFT context, one deals with strings that are described by a supersymmetric string action with D-brane boundary conditions moving in some curved space. In particular, there is no added point-particle action of the type we are considering here. However, AdS/CFT can still describe open strings that are dual to a quark and antiquark moving back-to-back with a flux tube forming in between. The resolution of the puzzle in this context is that the AdS/CFT dual involves a string that is falling in the AdS radial (holographic) direction. For a more detailed discussion, including some remarks about how AdS radial evolution can be dual to the parton shower, see Ref. [3].

$[-\varepsilon(t)/2, \varepsilon(t)/2]$. More generally, after a string breaking, the quark and antiquark will lose energy at different rates, so s ranges in $[-\varepsilon_1(t), \varepsilon_2(t)]$, with

$$\frac{d\varepsilon_1}{dt} = -\frac{1}{\sigma}\frac{dE_q}{dt} \tag{5.9}$$

$$\frac{d\varepsilon_2}{dt} = -\frac{1}{\sigma}\frac{dE_{\bar{q}}}{dt}. \tag{5.10}$$

We will denote $\varepsilon_1(t) + \varepsilon_2(t)$ simply by $\varepsilon(t)$, which measures the string energy in units of σ.

Numerically, it's more convenient to use a coordinate living in a fixed interval, $\tilde{s} = \frac{2(s+\varepsilon_1(t))}{\varepsilon(t)} - 1 \in [-1, 1]$. Because this new coordinate is a function of both the original s and $t = \tau$, the action will become more complicated: what was the derivative with respect to τ at fixed s, for instance, is now a combination of derivatives with respect to $\tilde{s}$ and τ:

$$\left.\frac{d\vec{X}}{d\tau}\right|_s = \left.\frac{d\vec{X}}{d\tilde{s}}\right|_\tau \frac{d\tilde{s}}{dt} + \left.\frac{d\vec{X}}{d\tau}\right|_{\tilde{s}}. \tag{5.11}$$

$$\frac{d\tilde{s}}{dt} = -2\frac{d\varepsilon}{dt}\frac{\tilde{s}+1}{\varepsilon} + \frac{2}{\varepsilon}\frac{d\varepsilon_1}{dt}. \tag{5.12}$$

Note that $\frac{d\tilde{s}}{dt}$ is interpolating between the rate of quark and antiquark energy change, in appropriate units, as we move along the string. Also note that the term $\left.\frac{d\vec{X}}{d\tilde{s}}\right|_\tau \frac{d\tilde{s}}{dt}$ accounts for the fact that the quark can have a velocity component $v_\parallel$ along the string direction, even though the string itself can carry only transverse momentum.

Thus we can rewrite the action (5.6) in the $(\tilde{s}, \tau)$ coordinate frame. It's somewhat ugly, as it involves $\varepsilon_{1,2}(\tau)$ and their time-derivatives, so in this parametrization there appears to be some nonlocal dependence on what is happening at the string endpoints. Nonetheless, the key point is that the change in string energy is entirely determined by the change in energy of the quark and antiquark, as in Eq. (5.8). Thus, numerically, we have a simple procedure to follow. We keep track of a fixed number N_{bit} of "string bits," i.e. locations at fixed intervals in $\tilde{s}$ along the string. In a small time interval dt, we can first calculate from Eqns. (5.7) and (5.8) the change in momentum and energy of the quark and antiquark at the ends of a string. This then tells us how $\varepsilon(t)$ is changing. We then use the equations of motion computed from the action Eq. (5.6), written in the $(\tilde{s}, \tau)$ frame and discretized, to evolve each "string bit" forward dt in time. In practice, we do this time evolution with a fourth-order Runge-Kutta algorithm. We then make small adjustments to the positions $\vec{X}(\tilde{s})$ and velocities $\partial_\tau \vec{X}(\tilde{s})$ of the string bits so that the parametrization conditions, Eqns. (5.4) and (5.5), are satisfied as precisely as possible numerically, because in practice small discretization errors in these conditions seem more numerically troublesome than discretization errors in the equations of motion themselves. This gives us a slightly crude, but fully relativistic, algorithm for evolving a configuration of strings forward in time.

The next step is to decay the strings. Here we use an *ad hoc* modification of the procedure from Section 5.2. We continue to be guided by the Schwinger calculation, but we are now taking it somewhat further from its domain of validity. Namely, we assume

that at a given instant in time, the decay probability of the string is proportional to the length of the string, and that the decay is equally likely to happen anywhere in the coordinate $\tilde{s}$. Rather than transverse momenta, we pull an energy from a Gaussian distribution, $dN(E) \sim d^2E \ \exp\left(-\frac{\pi E^2}{\sigma}\right)$, insisting that $E > 2m_q$, and remove a length of $\tilde{s}$ interval that balances this energy. In general this interval may also have some momentum. To construct the momenta of the new quark and antiquark, we boost to the rest frame of the removed string interval and construct the momenta of two daughters of mass m_q, perpendicular to the string direction at the center of the removed interval. (This ensures that in the case of the first breaking, this algorithm matches the simple semiclassical flux tube algorithm of our previous discussion.) Boosting back, we compute the components $v_\parallel$ and $v_\perp$ of the velocities of the new q and $\bar{q}$ and the corresponding rate of energy loss. We divide each daughter string into N_{bit} bits, just as the parent string had, interpolating between bits of the parent string to obtain the positions and velocities of the new bits. We place the final quark and antiquark at a location such that the constraint (5.5) is satisfied.

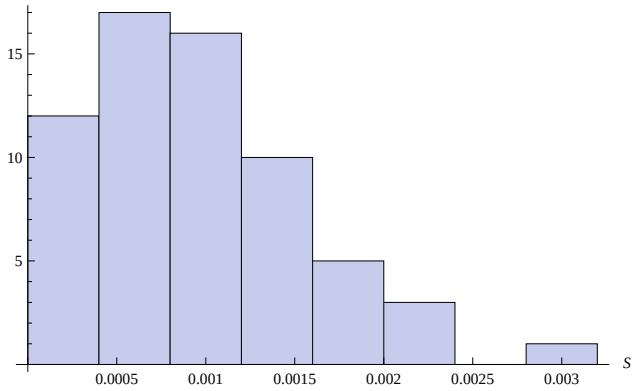

Figure 15: Sphericity distribution from the string model, after the first four string decays

The numerics of this procedure prove to be tricky, and we present results only for the first four decay steps. The results of this model are similar to those of the simpler static flux tube model. We have fixed $N_{bit} = 101$ for the number of points we track along the string, and have taken time steps of size 0.003125 GeV^{-1}. The quark mass is taken to be 0.3 GeV. Other parameters (tension, initial p_z, decay probability per unit time and unit length in string units) are as in the previous subsection. In Figure 15 we plot the sphericity distribution. It is peaked toward low values, showing that the string simulation predicts highly directional, jetty events just as our simpler flux tube model did.

6 Conclusions

We have examined various aspects of large N gauge theories for small and large 't Hooft coupling λ. We found that for small 't Hooft coupling agreement with perturbation theory suggests that the mass spectrum should asymptotically show the characteristic Regge-type

behavior rather than the KK-type scaling, that arises in the large λ limit. We have given a simple toy model that sheds light on how one can interpolate between these two spectra. This model suggests that the KK-like modes are more likely to be deeply bound mesons in the Coulombic short-distance part of the potential rather than genuine QCD-like modes related to the confining long distance potential. The event shapes resulting from scatterings in the small and large λ theories also seem to be qualitatively different. While for small λ one expects QCD-like events forming jets, for large λ we have shown that the final states are much more spherical, in agreement with the conjecture of Strassler and the calculations of Hofman and Maldacena for events in gravity duals of CFT's. We conclude that in order to fully capture the dynamics of QCD with small λ inclusion of some sort of stringy dynamics seems to be unavoidable.

Acknowledgments

We thank I. Klebanov, M. Luty, E. Pajer, and J. Thaler for useful discussions, and I. Klebanov and L. McAllister for comments on the manuscript. We thank the Aspen Center for Physics and the KITP in Santa Barbara for hospitality during the completion of this work. The research of C.C. is partly supported by the NSF under grant PHY-0355005 and by a US-Israeli BSF grant. J.T. is supported in part by the US Department of Energy under contract No. DE- FG03-91ER40674 and by a US-Israeli BSF grant.

Appendix

A Towards the completion of Migdal's program

In this appendix we describe an attempt at completing Migdal's program of analytically continuing the PT results for QCD into meromorphic functions valid for all energy regimes, along the lines of discussion in Sec. 2. This will lead us toward functions whose pole structure seems to asymptotically agree with that of the digamma function, however as we will see some other more exotic possibilities can not be completely ruled out based on our arguments.

Let us try to find a function that is a good fit to PT both in the deep Euclidean regime and the Minkowski regime away from the real axis (eg. also matches ρ_Δ for $\Delta \sim 1$). We will be looking for a meromorphic function of the form

$$\Pi_{MR}(s) = \sum_{n=1}^{\infty} \frac{r_n}{s - m_n^2}. \tag{A.1}$$

We require that this function (just as the Padé approximant) reproduces $\log s$ for $-s \gg 1$ with no $1/s$ corrections. But in addition we also require that it be a good fit to $\rho_\Delta(s)$ for $s > 1$. Let us first understand why the Padé approximation fails this requirement. The problem with the Padé approximation is that the succession of poles and residues obey

$m_n^2 \sim n^2$ and also $r_n \sim n$. The expression for ρ_Δ is

$$\rho_\Delta(s) = \sum_n \frac{r_n \Delta^2}{(s - m_n^2)^2 + \Delta^2}. \tag{A.2}$$

Clearly, for $s = m_n^2$ one gets a contribution of r_n, while the other terms are highly suppressed by the denominator. If $|r_n|$ is not asymptotically approaching a constant (or decreasing), then there is no way to correctly approximate for large n the asymptotically constant jump across the branch cut of the logarithm. Thus we conclude that the distribution of residues should be such that for large n r_n should be asymptotically bounded from above. This is the condition that the Padé approximant is not satisfying.

Now, we claim that this condition on the r_n in fact prohibits any function where the separation between poles grows asymptotically, not just the Padé approximant. For example, there is no function with a similar mass pattern $m_n^2 \sim n^2$ but with nonincreasing residues that provides a match to PT. This is intuitively clear: adding together functions supported on a narrow interval, growing progressively further apart, will never produce a constant. We can formalize this: take the average value of ρ_Δ between two consecutive poles m_n^2 and m_{n+1}^2. If ρ_Δ is to agree with PT, this average should not go to zero as $n \to \infty$. But we can just compute the average:

$$\bar{\rho}_{\Delta,n} \equiv \frac{1}{m_{n+1}^2 - m_n^2} \int_{m_n^2}^{m_{n+1}^2} ds \ \sum_k \frac{r_k \Delta^2}{(s - m_k^2)^2 + \Delta^2}. \tag{A.3}$$

Interchanging the order of summation and integration, this is just

$$\bar{\rho}_{\Delta,n} = \frac{1}{m_{n+1}^2 - m_n^2} \sum_k \frac{r_k}{\Delta} \left(\arctan \frac{m_k^2 - m_{n+1}^2}{\Delta} - \arctan \frac{m_k^2 - m_n^2}{\Delta} \right). \tag{A.4}$$

This expression is valid in general, regardless of the behavior of the m_n^2 and r_n.

Now we exploit the properties of the arctangent. If the distance between successive poles is asymptotically growing, we can choose n such that $\frac{m_{n+1}^2 - m_n^2}{\Delta} \gg 1$. Then we use the fact that:

$$\arctan(x) - \arctan(x - x_0) \approx \pi \theta(x) \theta(x_0 - x), \quad x_0 \gg 1. \tag{A.5}$$

In other words, for very large values of x_0 this function is approximately π on the interval from 0 to x_0 and 0 outside that interval. In particular, in our case we identify x with $\frac{m_k^2 - m_{n+1}^2}{\Delta}$ and x_0 with $\frac{m_{n+1}^2 - m_n^2}{\Delta}$. It is then clear that the only k values that contribute to the sum in Eq. A.4 are $k = n + 1$ and $k = n$. The result is that

$$\bar{\rho}_{\Delta,n} \approx \frac{1}{m_{n+1}^2 - m_n^2} \frac{(r_n + r_{n+1}) \arctan(m_{n+1}^2 - m_n^2)}{\Delta}. \tag{A.6}$$

We have argued that the r_n are not asymptotically growing; the arctangent is also bounded (it is approximately π). Hence, if the denominator $m_{n+1}^2 - m_n^2$ is growing, this expression tends asymptotically to zero at large n, in contradiction with PT.

At this point we have established that the radial Regge physics, $m_n^2 \sim n$ asymptotically, is the behavior which matches PT with the fewest poles on a given interval. We do not have an argument that we cannot have slower growth, for instance $m_n^2 \sim \sqrt{n}$. Intuitively it is apparent that if we *do* have slower growth, the residues must decrease or we will construct a function that greatly exceeds the perturbative answer at large s. Let's see what happens if we attempt to extend the above argument to the case of poles that grow successively closer. In that case we are interested in the opposite limit of the difference of arctangents, $x_0 \to 0$. This is of course determined by the derivative:

$$\arctan(x) - \arctan(x - x_0) \approx \frac{x_0}{x^2+1}, \quad x_0 \ll 1. \tag{A.7}$$

Assuming the separation between poles is decreasing with n, we can choose n such that $\frac{m_{n+1}^2 - m_n^2}{\Delta} \ll 1$ and the above formula is valid. Note that $\frac{x_0}{x^2+1} > \frac{x_0}{2}$ provided $|x| < 1$. Again identifying x with $\frac{m_k^2 - m_{n+1}^2}{\Delta}$ and summing only over the terms where $|x| < 1$, we find that the sum is *at least*

$$\bar{\rho}_{\Delta,n} \gtrsim \frac{1}{m_{n+1}^2 - m_n^2} \sum_{k:\ |m_n^2 - m_k^2| < \Delta} \frac{r_k}{\Delta} \frac{m_{n+1}^2 - m_n^2}{2\Delta} = \frac{1}{2\Delta^2} \sum_{k:\ |m_n^2 - m_k^2| < \Delta} r_k. \tag{A.8}$$

From this we get an estimate of how quickly the residues r_k must decrease: fast enough to compensate for the number of poles in a given interval. Assuming m_n^2 is a smooth function of n, for large n the number of poles in a unit interval is characterized by $(m_{n+1}^2 - m_n^2)^{-1}$, so the residue should satisfy $r_n \approx m_{n+1}^2 - m_n^2$.

Now, since we don't have any argument against decreasing poles, it seems possible that a function like

$$\Pi(s) = \sum_n \left(\frac{1}{\sqrt{n}(s - \sqrt{n})} + \frac{1}{n} \right) \tag{A.9}$$

could provide a good match to PT. We have numerically investigated this, and indeed such a function appears to agree well. It does not seem possible to determine the correct behavior of the distribution of poles just from matching the leading perturbative behavior of two-point functions. On the other hand, the asymptotically constant distribution of pole expected from Regge physics is in some sense the *minimal* choice, so in the absence of other arguments it seems preferable.

B Lorentz Invariance of Flux tube Breaking

Here we show that for center of mass energies much larger than the the typical transverse momentum $\sqrt{\sigma}$, the simple model of Section 5.2 gives a Lorentz invariant description of the early decays of a flux tube. At large enough center of mass energies the flux tube stretches in a straight line between the back-to-back quark and anti-quark, and the transverse momenta are negligible. In this limit, the situation reduces to a 1+1 dimensional problem. The discussion can be further simplified by noting that the pair production which breaks the flux

tube is just like 2D bubble nucleation, which is Lorentz invariant around the center of the bubble [60–62].

Let us take the string axis to be along the x direction, and our string breaking pair production to be centered at $x = 0$, $t = 0$, which means that the original production of the flux tube took place at some earlier (negative) time. At $t = 0$, we will take a quark of mass m to be at $x = x_0$ and moving in the positive x direction with momentum p_0; the anti-quark at the other end of the flux tube is somewhere along the negative x axis moving in the negative x direction. The Nambu-Goto-quark equations of motion (5.7) tell us that the momentum of the quark will decrease linearly with time:

$$p_q = p_0 - \sigma t \ . \tag{B.10}$$

When the flux tube breaks, a new quark—anti-quark pair is formed at $t = 0$. Neglecting the small transverse momentum, the new pair is at rest, and in order to conserve energy, a section of the flux tube must be removed to account for their rest energy. Thus the new anti-quark of mass m is at

$$x = d = m/\sigma \tag{B.11}$$

while the new quark is at $x = -d$, so that the flux tube section from $-d$ to d has donated its energy to provide the new masses. Again the Nambu-Goto-quark equations of motion (5.7) tell us that the subsequent momentum of the new anti-quark is given by

$$p_a = \sigma t \ . \tag{B.12}$$

Integrating the velocity, $v_a = p_a/E_a$, of the new anti-quark we find that its subsequent position is

$$x_a = \int v_a \, dt = \int \frac{p_a}{\sqrt{m^2 + p_a^2}} \, dt = \sqrt{d^2 + t^2} \ . \tag{B.13}$$

This is, of course, exactly what we expect from 2D bubble nucleation: the trajectory should be an hyperboloid, corresponding to a circle in Euclidean space ($x^2 + t_E^2 = d^2$). Similarily, the trajectory of the original quark can be found by integration as well but the result just corresponds to another circle in Euclidean space, $(x - x_c)^2 + (t_E - t_c)^2 = d^2$, however one that is not centered about the origin. The center is given by

$$x_c = x_0 + \frac{\sqrt{m^2 + p_0^2}}{\sigma} = x_0 + \sqrt{d^2 + \frac{p_0^2}{\sigma^2}} \ , \tag{B.14}$$

$$t_c = \frac{p_0}{\sigma} \ . \tag{B.15}$$

Thus the position of the quark is simply given by

$$x_q = x_c - \sqrt{d^2 + (t_c - t)^2} \ . \tag{B.16}$$

Now let us calculate the rest mass of the daughter flux tube. This is simple at $t = 0$. The total momentum is just that of the quark (since a string cannot carry longitudinal momentum), so $p = p_0$. The total energy is

$$E = m + \sigma(x_0 - d) + \sqrt{m^2 + p_0^2} = \sigma\, x_0 + \sqrt{m^2 + p_0^2}\ . \tag{B.17}$$

Thus the rest mass is

$$m_{rest} = \sqrt{E^2 - p^2} = \sqrt{m^2 + \sigma^2 x_0^2 + 2\sigma x_0 \sqrt{m^2 + p_0^2}}\ . \tag{B.18}$$

What if we had chosen to calculate the rest mass in some other frame? The issue may seem quite complex since a boost will change the length of the string, but the string length is changing with time so the new time slicing will actually involve the string ends at different stages of evolution. However the situation is really quite simple. If we boost to a frame moving with velocity v to the right, special relativity tells us that in that frame the energy and momentum will be

$$E' = \gamma(E - v p_0); \quad p' = \gamma(p_0 - v E)\ . \tag{B.19}$$

Since the new anti-quark trajectory is boost invariant it will be at $x' = d$ at $t' = 0$, so in analogy to Eq. (B.17) we should also have that at $t' = 0$ the total energy in this frame is

$$E' = \sigma\, x'_q + \sqrt{m^2 + p'^2}\ , \tag{B.20}$$

where x'_q is the position of the quark in the boosted frame at $t' = 0$. Comparing Eqs. (B.19) and (B.20) tells us what x'_q should be if the model is Lorentz invariant. We can independently calculate x'_q from the boost of the quark trajectory. This is most easily done by rotating the center of the corresponding circle in Euclidean space (which is equivalent to boosting the the focus of the hyperboloid in Minkowski space). This gives, at $t' = 0$,

$$x'_q = \gamma\,(x_c - v\, t_c) - \sqrt{d^2 + \gamma^2\,(t_c - v\, x_c)^2}\ , \tag{B.21}$$

which is exactly what is required for Eqs. (B.19) and (B.20) to agree. Thus the rest mass of the daughter flux tube is the same in any boosted frame, and the model is indeed Lorentz invariant.

References

[1] J. M. Maldacena, Adv. Theor. Math. Phys. **2**, 231 (1998) [Int. J. Theor. Phys. **38**, 1113 (1999)] [`hep-th/9711200`]; S. S. Gubser, I. R. Klebanov and A. M. Polyakov, Phys. Lett. B **428**, 105 (1998) [arXiv:hep-th/9802109]. E. Witten, Adv. Theor. Math. Phys. **2**, 253 (1998) [`hep-th/9802150`].

[2] J. Erlich, E. Katz, D. T. Son and M. A. Stephanov, `hep-ph/0501128`; L. Da Rold and A. Pomarol, `hep-ph/0501218`.

[3] M. J. Strassler, arXiv:0801.0629 [hep-ph].

[4] J. Polchinski and M. J. Strassler, JHEP **0305**, 012 (2003) [arXiv:hep-th/0209211].

[5] D. M. Hofman and J. Maldacena, JHEP **0805**, 012 (2008) [arXiv:0803.1467 [hep-th]].

[6] Y. Hatta, E. Iancu and A. H. Mueller, JHEP **0805**, 037 (2008) [arXiv:0803.2481 [hep-th]]

[7] Y. Hatta, E. Iancu and A. H. Mueller, JHEP **0801**, 063 (2008) [arXiv:0710.5297 [hep-th]]; Y. Hatta and T. Matsuo, arXiv:0804.4733 [hep-th]; Y. Hatta and T. Matsuo, arXiv:0807.0098 [hep-ph]; Y. Hatta, arXiv:0810.0889 [hep-ph].

[8] G. 't Hooft, Nucl. Phys. B **72**, 461 (1974).

[9] L. Randall and R. Sundrum, Phys. Rev. Lett. **83**, 3370 (1999) [arXiv:hep-ph/9905221].

[10] I. R. Klebanov and M. J. Strassler, JHEP **0008**, 052 (2000) [arXiv:hep-th/0007191].

[11] G. 't Hooft, Nucl. Phys. B **138**, 1 (1978).

[12] K. G. Wilson, Phys. Rev. D **10**, 2445 (1974); Y. Nambu, Phys. Rev. D **10**, 4262 (1974). Y. Nambu, Phys. Lett. B **80**, 372 (1979); M. Luscher, G. Munster and P. Weisz, Nucl. Phys. B **180**, 1 (1981); M. Luscher, Nucl. Phys. B **180**, 317 (1981); R. Sundrum, arXiv:hep-ph/9702306.

[13] A. Armoni, J. L. F. Barbon and A. C. Petkou, JHEP **0210**, 069 (2002) [arXiv:hep-th/0209224]; L. A. Pando Zayas, J. Sonnenschein and D. Vaman, Nucl. Phys. B **682**, 3 (2004) [arXiv:hep-th/0311190]; F. Bigazzi, A. L. Cotrone, L. Martucci and L. A. Pando Zayas, Phys. Rev. D **71**, 066002 (2005) [arXiv:hep-th/0409205]; M. Kruczenski, L. A. P. Zayas, J. Sonnenschein and D. Vaman, JHEP **0506**, 046 (2005) [arXiv:hep-th/0410035].

[14] J. M. Pons, J. G. Russo and P. Talavera, Nucl. Phys. B **700**, 71 (2004) [arXiv:hep-th/0406266].

[15] E. Witten, Adv. Theor. Math. Phys. **2**, 505 (1998) [arXiv:hep-th/9803131].

[16] C. Csaki, H. Ooguri, Y. Oz and J. Terning, JHEP **9901**, 017 (1999) [arXiv:hep-th/9806021]; H. Ooguri, H. Robins and J. Tannenhauser, Phys. Lett. B **437**, 77 (1998) [arXiv:hep-th/9806171].

[17] M. Kruczenski, D. Mateos, R. C. Myers and D. J. Winters, JHEP **0307**, 049 (2003) [arXiv:hep-th/0304032].

[18] S. Hong, S. Yoon and M. J. Strassler, JHEP **0404**, 046 (2004) [arXiv:hep-th/0312071].

[19] T. Sakai and J. Sonnenschein, JHEP **0309**, 047 (2003) [arXiv:hep-th/0305049]; J. Babington, J. Erdmenger, N. J. Evans, Z. Guralnik and I. Kirsch, Phys. Rev. D **69**, 066007 (2004) [arXiv:hep-th/0306018]; S. Hong, S. Yoon and M. J. Strassler, JHEP **0604**, 003 (2006) [arXiv:hep-th/0409118]; J. Erdmenger, N. Evans, I. Kirsch and E. Threlfall, Eur. Phys. J. A **35**, 81 (2008) [arXiv:0711.4467 [hep-th]].

[20] M. Berg, M. Haack and W. Mueck, Nucl. Phys. B **789**, 1 (2008) [arXiv:hep-th/0612224]; M. K. Benna, A. Dymarsky, I. R. Klebanov and A. Solovyov, JHEP **0806**, 070 (2008) [arXiv:0712.4404 [hep-th]].

[21] D. T. Son and M. A. Stephanov, Phys. Rev. D **69**, 065020 (2004) [arXiv:hep-ph/0304182].

[22] E. G. Gimon, L. A. Pando Zayas, J. Sonnenschein and M. J. Strassler, JHEP **0305**, 039 (2003) [arXiv:hep-th/0212061].

[23] S. Hong, S. Yoon and M. J. Strassler, JHEP **0603**, 012 (2006) [arXiv:hep-th/0410080].

[24] O. Aharony, S. Minwalla and T. Wiseman, Class. Quant. Grav. **23**, 2171 (2006) [arXiv:hep-th/0507219].

[25] I. R. Klebanov, J. M. Maldacena and C. B. . Thorn, JHEP **0604**, 024 (2006) [arXiv:hep-th/0602255]; R. C. Brower, C. I. Tan and C. B. Thorn, Phys. Rev. D **73**, 124037 (2006) [arXiv:hep-th/0603256].

[26] J. Polchinski and M. J. Strassler, Phys. Rev. Lett. **88**, 031601 (2002) [arXiv:hep-th/0109174]; R. C. Brower, J. Polchinski, M. J. Strassler and C. I. Tan, JHEP **0712**, 005 (2007) [arXiv:hep-th/0603115]; R. C. Brower, M. J. Strassler and C. I. Tan, arXiv:0710.4378 [hep-th].

[27] L. Cornalba, M. S. Costa, J. Penedones and R. Schiappa, JHEP **0708**, 019 (2007) [arXiv:hep-th/0611122]; L. Cornalba, M. S. Costa, J. Penedones and R. Schiappa, Nucl. Phys. B **767**, 327 (2007) [arXiv:hep-th/0611123]; L. Cornalba, M. S. Costa and J. Penedones, JHEP **0709**, 037 (2007) [arXiv:0707.0120 [hep-th]]; L. Cornalba, M. S. Costa and J. Penedones, JHEP **0806**, 048 (2008) [arXiv:0801.3002 [hep-th]]; L. Cornalba and M. S. Costa, arXiv:0804.1562 [hep-ph].

[28] M. Unsal, arXiv:0807.0466 [hep-th].

[29] T. Sakai and S. Sugimoto, Prog. Theor. Phys. **113**, 843 (2005) [arXiv:hep-th/0412141].

[30] C. Vafa and E. Witten, Nucl. Phys. B **431**, 3 (1994) [arXiv:hep-th/9408074]; N. Dorey, JHEP **9907**, 021 (1999) [arXiv:hep-th/9906011]; N. Dorey and S. P. Kumar, JHEP **0002**, 006 (2000) [arXiv:hep-th/0001103]

[31] J. Polchinski and M. J. Strassler, arXiv:hep-th/0003136.

[32] A. A. Migdal, Annals Phys. **109**, 365 (1977).

[33] M. Shifman, arXiv:hep-ph/0507246.

[34] J. Erlich, G. D. Kribs and I. Low, arXiv:hep-th/0602110; A. Falkowski and M. Perez-Victoria, JHEP **0702**, 086 (2007) [arXiv:hep-ph/0610326].

[35] B. Blok, M. A. Shifman and D. X. Zhang, Phys. Rev. D **57**, 2691 (1998) [Erratum-ibid. D **59**, 019901 (1999)] [arXiv:hep-ph/9709333]; M. A. Shifman, arXiv:hep-ph/0009131.

[36] E. C. Poggio, H. R. Quinn and S. Weinberg, Phys. Rev. D **13**, 1958 (1976).

[37] M. Golterman and S. Peris, Phys. Rev. D **67**, 096001 (2003) [arXiv:hep-ph/0207060]; O. Cata, Phys. Rev. D **75**, 106004 (2007) [arXiv:hep-ph/0605251]; J. Mondejar and A. Pineda, JHEP **0710**, 061 (2007) [arXiv:0704.1417 [hep-ph]]; P. Masjuan and S. Peris, JHEP **0705**, 040 (2007) [arXiv:0704.1247 [hep-ph]].

[38] A. P. Szczepaniak and E. S. Swanson, Phys. Rev. D **65**, 025012 (2002) [arXiv:hep-ph/0107078]; A. P. Szczepaniak and E. S. Swanson, Phys. Lett. B **577**, 61 (2003) [arXiv:hep-ph/0308268]; N. Ligterink and E. S. Swanson, Phys. Rev. C **69**, 025204 (2004) [arXiv:hep-ph/0310070].

[39] S. J. Rey and J. T. Yee, Eur. Phys. J. C **22**, 379 (2001) [arXiv:hep-th/9803001]; J. M. Maldacena, Phys. Rev. Lett. **80**, 4859 (1998) [arXiv:hep-th/9803002].

[40] D. Zwanziger, Phys. Rev. Lett. **90**, 102001 (2003) [arXiv:hep-lat/0209105].

[41] H. Boschi-Filho, N. R. F. Braga and C. N. Ferreira, Phys. Rev. D **73**, 106006 (2006) [Erratum-ibid. D **74**, 089903 (2006)] [arXiv:hep-th/0512295]; H. Boschi-Filho, N. R. F. Braga and C. N. Ferreira, arXiv:hep-th/0610131.

[42] O. Andreev, Phys. Rev. D **73**, 107901 (2006) [arXiv:hep-th/0603170].

[43] O. Andreev and V. I. Zakharov, Phys. Rev. D **74**, 025023 (2006) [arXiv:hep-ph/0604204]. C. D. White, Phys. Lett. B **652**, 79 (2007) [arXiv:hep-ph/0701157]. F. Giannuzzi, arXiv:0810.2736 [hep-ph].

[44] J. D. Bjorken and S. J. Brodsky, Phys. Rev. D **1**, 1416 (1970).

[45] A. Karch, E. Katz, D. T. Son and M. A. Stephanov, Phys. Rev. D **74**, 015005 (2006) [arXiv:hep-ph/0602229].

[46] C. Csáki and M. Reece, JHEP **0705**, 062 (2007) [arXiv:hep-ph/0608266]. U. Gursoy and E. Kiritsis, JHEP **0802**, 032 (2008) [arXiv:0707.1324 [hep-th]]. U. Gursoy, E. Kiritsis and F. Nitti, JHEP **0802**, 019 (2008) [arXiv:0707.1349 [hep-th]]. B. Batell and T. Gherghetta, Phys. Rev. D **78**, 026002 (2008) [arXiv:0801.4383 [hep-ph]]. W. de Paula, T. Frederico, H. Forkel and M. Beyer, arXiv:0806.3830 [hep-ph].

[47] E. Katz and T. Okui, arXiv:0710.3402 [hep-th].

[48] S. J. Brodsky and G. F. de Teramond, Phys. Lett. B **582**, 211 (2004) [arXiv:hep-th/0310227]; G. F. de Teramond and S. J. Brodsky, Phys. Rev. Lett. **94**, 201601 (2005) [arXiv:hep-th/0501022]; S. J. Brodsky and G. F. de Teramond, Phys. Rev. Lett. **96**, 201601 (2006) [arXiv:hep-ph/0602252].

[49] G. F. Chew and S. C. Frautschi, Phys. Rev. Lett. **8**, 41 (1962); J. R. Forshaw and D. A. Ross, Cambridge Lect. Notes Phys. **9**, 1 (1997).

[50] K. J. Juge, J. Kuti and C. Morningstar, Phys. Rev. Lett. **90**, 161601 (2003) [arXiv:hep-lat/0207004].

[51] A. Casher, H. Neuberger and S. Nussinov, Phys. Rev. D **20**, 179 (1979).

[52] N. K. Glendenning and T. Matsui, Phys. Rev. D **28**, 2890 (1983).

[53] E. G. Gurvich, Phys. Lett. B **87**, 386 (1979).

[54] N. Isgur and J. E. Paton, Phys. Lett. B **124**, 247 (1983); N. Isgur and J. E. Paton, Phys. Rev. D **31**, 2910 (1985); R. Kokoski and N. Isgur, Phys. Rev. D **35**, 907 (1987).

[55] B. Andersson, G. Gustafson, G. Ingelman and T. Sjostrand, Phys. Rept. **97**, 31 (1983).

[56] J. Greensite and C. B. Thorn, JHEP **0202**, 014 (2002) [arXiv:hep-ph/0112326].

[57] J. Greensite, Prog. Part. Nucl. Phys. **51**, 1 (2003) [arXiv:hep-lat/0301023].

[58] B. Zwiebach, *A First Course in String Theory.* Cambridge, UK: Univ. Pr. (2004) 558 p

[59] J. Kang and M. A. Luty, arXiv:0805.4642 [hep-ph].

[60] S. R. Coleman, Phys. Rev. D **15** (1977) 2929 [Erratum-ibid. D **16** (1977) 1248]; C. G. . Callan and S. R. Coleman, Phys. Rev. D **16** (1977) 1762; S. R. Coleman, "The Uses of Instantons", in *Aspects of Symmetry: Selected Erice Lectures* (Cambridge University Press, Cambridge, 1985).

[61] A. Casher, H. Neuberger and S. Nussinov, Phys. Rev. D **21** (1980) 1966.

[62] V. Barger and R. Phillips, p. 184 *Collider Physics* (Westview Press, Boulder CO, 1991).